AIMS Mathematics, 8(1): 264–284.
DOI: 10.3934/math.2023012
Received: 28 June 2022
Revised: 31 August 2022
Accepted: 01 September 2022
Published: 28 September 2022

http://www.aimspress.com/journal/Math

Research article

Energy analysis of the ADI-FDTD method with fourth-order accuracy in time for Maxwell's equations

Li Zhang[1,2,*], **Maohua Ran**[2,3] **and Hanyue Zhang**[2]

[1] V. C. & V. R. Key Lab of Sichuan Province, Sichuan Normal University, Chengdu 610068, China

[2] School of Mathematical Science, Sichuan Normal University, Chengdu 610068, China

[3] School of Mathematics, Aba Teachers University, Aba 623002, China

* **Correspondence:** Email: lizhang_hit@163.com.

Abstract: In this work, the ADI-FDTD method with fourth-order accuracy in time for the 2-D Maxwell's equations without sources and charges is proposed. We mainly focus on energy analysis of the proposed ADI-FDTD method. By using the energy method, we derive the numerical energy identity of the ADI-FDTD method and show that the ADI-FDTD method is approximately energy-preserving. In comparison with the energy in theory, the numerical one has two perturbation terms and can be used in computation in order to keep it approximately energy-preserving. Numerical experiments are given to show the performance of the proposed ADI-FDTD method which confirm the theoretical results.

Keywords: Maxwell's equations; ADI-FDTD; energy method; approximately energy-preserving
Mathematics Subject Classification: 65M06, 65N15

1. Introduction

Maxwell's equations are very important partial differential equations and they play a significant role in electromagnetic theory. Numerical solutions for Maxwell's equations are extensive in science and engineering, for example, for radio-frequencies, antennas, microwaves, wireless engineering and the design of CPUs in microelectronics. There are many efficient numerical methods for solving Maxwell's equations, such as the finite-difference time-domain (FDTD) method [1, 2], the finite element method [3], the weak Galerkin finite element method [4] and so on.

The FDTD method (also called Yee′s scheme) was first introduced by Yee [1] in 1966, and later applied to many problems in computational electromagnetics [5–19]. However, the traditional FDTD method is conditionally stable and must satisfy the Courant-Friedrichs-Lewy (CFL) stability condition;

see [5, 20–22]. For the 2-D Maxwell's problem, the CFL condition is

$$c\Delta t \leq [\frac{1}{(\Delta x)^2} + \frac{1}{(\Delta y)^2}]^{-\frac{1}{2}},$$

where c is the maximum of the wave velocity, i.e., the speed of light in vacuum, Δt is the time step size and Δx and Δy are the spatial step sizes. This implies that the maximum time step size is limited by the minimum spatial size, and that computation of the FDTD method needs much CPU time when the spatial step sizes are small.

Many numerical methods have been proposed for Maxwell's equations to get rid of this restriction. One of these methods is the alternating direction implicit FDTD method, which was proposed in 1999 by Namiki [2] and which zheng et al. [12] proved to be unconditionally stable. The ADI-FDTD scheme consists of two stages and can be solved directly by using the Thomas algorithm, since each stage includes tri-diagonal systems of linear equations. By truncation error analysis, it was found that this method has second-order accuracy in both time and space. The ADI-FDTD method is quickly applied to various electromagnetic computations and the ADI-FDTD methods with high-order accuracy were developed. Based on Yoshida's work [9], Tan and Ding [23] proposed a new ADI-FDTD method with fourth-order accuracy in time for 2D-wave propagation in a lossless, isotropic medium. The new ADI-FDTD method was proved to be unconditionally stable by the Fourier method, i.e., this method is free from the constraints of the CFL conditions. However, energy analysis of the new method in terms of energy preservation and convergence are not available.

Analysis of the energy of the methods and construction of energy-preserving methods are popular and valuable. As Li and Vu-Quoc said in [10], to some extent, the ability to preserve some invariant properties of the original differential equation is a criterion to judge the success of a numerical simulation. Therefore, it is important to develop energy-preserving algorithms and analyze the energy of existing algorithms for solving Maxwell's equations. It is well known that the FDTD method is a popular numerical method in computational electromagnetics, but it is not unconditionally stable and fails to satisfy the energy conservation property. In order to make up for these shortcomings, various energy-preserving methods have been applied to solve Maxwell's equations based on the ADI and splitting techniques. For example, a new splitting FDTD scheme for Maxwell's equations was proposed in [24]. It proved that the new scheme was unconditionally stable and energy-preserving. Furthermore, Chen et al. [25] proposed the symmetric energy-conserved splitting FDTD scheme (i.e., symmetric EC-S-FDTD). It was proved that this symmetric EC-S-FDTD method is unconditionally stable and has second-order convergence in both time and space. In [26], a symmetric EC-S-FDTD method for Maxwell's equations in negative index metamaterials was proposed. We note that these works are limited to cases with homogeneous boundary conditions. In addition, a proper summation by parts (SBP) formula was found for the approximate derivative in [27]. A "simultaneous approximation term" was used to treat the inhomogeneous boundary conditions. Appel*ö* and Bokil [28] presented the construction of novel SBP-FDTD methods for the numerical discretization of the Maxwell-Duffing models and derived energy estimates for the semi-discrete methods that are analogous to the continuous energy estimates. Boundary and interface conditions were handled by the simultaneous approximation technique. In [29], a new framework to construct time-stable finite-difference schemes was proposed for hyperbolic systems base on the application of strong boundary conditions. Sufficient conditions for strong time stability and conservation were derived for the linear advection equation

and coupled system of hyperbolic equations using the energy method. For other energy-preserving methods of Maxwell's equations, please see the relevant references [30–33]. In quantum mechanics, the conservative methods are also favored by researchers; see [34–38].

In this paper, we consider the following 2-D transverse electric (TE) problem in a lossless medium and without sources and charges:

$$\frac{\partial E_x}{\partial t} = \frac{1}{\varepsilon}\frac{\partial H_z}{\partial y}, \tag{1.1}$$

$$\frac{\partial E_y}{\partial t} = -\frac{1}{\varepsilon}\frac{\partial H_z}{\partial x}, \tag{1.2}$$

$$\frac{\partial H_z}{\partial t} = \frac{1}{\mu}\left(\frac{\partial E_x}{\partial y} - \frac{\partial E_y}{\partial x}\right) \tag{1.3}$$

with $(x, y) \in \Omega = [0, a] \times [0, b]$ and $t \in (0, T]$, where ε is the electric permittivity of the medium, μ is the magnetic permeability and $\mathbf{E} = (E_x(x, y, t), E_y(x, y, t))$ and $H_z = H_z(x, y, t)$ are the electric field and the magnetic field, respectively.

Motivated by Tan and Ding [23], we present a ADI-FDTD scheme with fourth-order accuracy in time for the TE problems (1.1)–(1.3), and an analysis of the energy of the scheme. We use the energy method to derive the numerical energy identity of this method. It is found that the method is approximately energy-preserving. In addition, numerical experiments are provided to verify the numerical performance of the ADI-FDTD scheme with fourth-order accuracy in time.

The remaining part of the paper is organized as follows. In Section 2, we introduce some preliminaries and notations. In Section 3, we give the detailed energy analysis of the scheme. In Section 4, we present some numerical results to illustrate the accuracy, convergence and energy identity of the scheme.

2. Preliminaries and notations

We consider the perfectly electric conductor (PEC) boundary condition as follows:

$$(\mathbf{E}, 0) \times (\vec{\mathbf{n}}, 0) = 0, \text{on } (0, T] \times \partial\Omega, \tag{2.1}$$

where $\partial\Omega$ denotes the boundary of Ω and $\vec{\mathbf{n}}$ is the outward normal vector on $\partial\Omega$. The initial conditions are

$$\mathbf{E}(\mathbf{x}, \mathbf{y}, \mathbf{0}) = \mathbf{E_0}(\mathbf{x}, \mathbf{y}) = (E_{x0}(x, y), E_{y0}(x, y)), H_z(x, y, 0) = H_{z0}(x, y). \tag{2.2}$$

It is well known that for suitably smooth data, the problem has a unique solution for all time; see [8]. Here, we assume that the solution of the Maxwell's equations (1.1)–(1.3) has the following regularity property:

$$\mathbf{E} \in C((0, T], [C^3(\bar{\Omega})]^2) \cap C^1([0, T], [C^1(\bar{\Omega})]^2) \cap C^2([0, T], [C(\bar{\Omega})]^2), \tag{2.3}$$

$$H_z \in C((0, T], [C^3(\bar{\Omega})]) \cap C^1([0, T], [C^1(\bar{\Omega})]) \cap C^2([0, T], [C(\bar{\Omega})]). \tag{2.4}$$

To simplify the notations we only consider the case of constant coefficients which are independent of x and y. But the proposed method is valid for the case of variable coefficients with $\varepsilon = \varepsilon(x, y)$ and $\mu = \mu(x, y)$.

For the problems in a lossless medium, Poynting's theorem states that electromagnetic energy stays constant for all time. The following lemma is an integral form of the Poynting's theorem.

Lemma 2.1. *[24] If* $\boldsymbol{E}$ *and* $\boldsymbol{H}$ *are the solutions of the Maxwell's equations* (1.1)–((1.3) *in a lossless medium and satisfy the PEC boundary condition* (2.1)*, then for any* $t \geq 0$*, it holds that*

$$\int_\Omega (\epsilon|\boldsymbol{E}(x,t)|^2 + \mu|\boldsymbol{H}(x,t)|^2)dxdy \equiv \int_\Omega (\epsilon|\boldsymbol{E}(x,0)|^2 + \mu|\boldsymbol{H}(x,0)|^2)dxdy.$$

Consider the space domain $\Omega = [0,a] \times [0,b]$ and time interval [0,T]. Let $\Delta x > 0$ and $\Delta y > 0$ be space steps and $\Delta t > 0$ be the time step; define

$$\begin{aligned} 0 = x_0 \leq x_1 \leq \cdots \leq x_i \leq \cdots \leq x_I = a, \\ 0 = y_0 \leq y_1 \leq \cdots \leq y_j \leq \cdots \leq y_J = b, \\ 0 = t_0 \leq t_1 \leq \cdots \leq t_n \leq \cdots \leq t_N = T, \end{aligned}$$

where $0 \leq i \leq I, 0 \leq j \leq J$ and $0 \leq n \leq N$; I, J and N are integers. Define $(x_\alpha, y_\beta, t^\theta) = (\alpha\Delta x, \beta\Delta y, \theta\Delta t)$, where α is either i or $i+\frac{1}{2}$, β is either j or $j+\frac{1}{2}$ and θ is either n or $n+\frac{1}{2}$. For a function $F(x,y,t)$, define

$$F^m_{\alpha,\beta} = F(\alpha\Delta x, \beta\Delta y, m\Delta t), \quad \delta_t F^m_{\alpha,\beta} = \frac{F^{m+\frac{1}{2}}_{\alpha,\beta} - F^{m-\frac{1}{2}}_{\alpha,\beta}}{\Delta t}, \tag{2.5}$$

$$\delta_x F^m_{\alpha,\beta} = \frac{F^m_{\alpha+\frac{1}{2},\beta} - F^m_{\alpha-\frac{1}{2},\beta}}{\Delta x}, \quad \delta_y F^m_{\alpha,\beta} = \frac{F^m_{\alpha,\beta+\frac{1}{2}} - F^m_{\alpha,\beta-\frac{1}{2}}}{\Delta y}, \tag{2.6}$$

and $\delta_u\delta_v F^m_{\alpha,\beta} = \delta_u(\delta_v F^m_{\alpha,\beta})$ where $u, v \in \{x, y\}$.

Denote by $E^m_{x_{i+\frac{1}{2},j}}$, $E^m_{y_{i,j+\frac{1}{2}}}$ and $H^m_{z_{i+\frac{1}{2},j+\frac{1}{2}}}$ the approximations of the electric field $E_x(i+\frac{1}{2}, j, t^m)$, $E_y(i, j+\frac{1}{2}, t^m)$ and $H_z(i+\frac{1}{2}, j+\frac{1}{2}, t^m)$, respectively. For a grid function $F_{\alpha,\beta}$, where $\alpha = i, i+\frac{1}{2}$ and $\beta = j, j+\frac{1}{2}$, define the discrete L^2 norms:

$$\|F\|^2_{E_x} = \sum_{i=0}^{I-1}\sum_{j=1}^{J-1} \varepsilon(F_{i+\frac{1}{2},j})^2\Delta x\Delta y, \quad \|F\|^2_{E_y} = \sum_{i=1}^{I-1}\sum_{j=0}^{J-1} \varepsilon(F_{i,j+\frac{1}{2}})^2\Delta x\Delta y, \tag{2.7}$$

$$\|F\|^2_{H_z} = \sum_{i=0}^{I-1}\sum_{j=0}^{J-1} \mu(F_{i+\frac{1}{2},j+\frac{1}{2}})^2\Delta x\Delta y, \quad \|F\|^2_{\delta_x E_y} = \sum_{i=1}^{I-2}\sum_{j=0}^{J-1} \varepsilon(F_{i+\frac{1}{2},j+\frac{1}{2}})^2\Delta x\Delta y, \tag{2.8}$$

$$\|F\|^2_{\delta_x H_z} = \sum_{i=1}^{I-1}\sum_{j=0}^{J-1} \mu(F_{i,j+\frac{1}{2}})^2\Delta x\Delta y, \quad \|F\|^2_{\delta_y E_x} = \sum_{i=0}^{I-1}\sum_{j=1}^{J-2} \varepsilon(F_{i+\frac{1}{2},j+\frac{1}{2}})^2\Delta x\Delta y, \tag{2.9}$$

$$\|F\|^2_{\delta_y H_z} = \sum_{i=0}^{I-1}\sum_{j=1}^{J-1} \mu(F_{i+\frac{1}{2},j})^2\Delta x\Delta y. \tag{2.10}$$

For a grid function $\mathbf{F} = (U, V)$ over the mesh for the electric field, the L^2 norms of the vector-valued function is defined as follows:

$$\|\mathbf{F}\|^2_E = \|U\|^2_{E_x} + \|V\|^2_{E_y}.$$

Now we give the ADI-FDTD scheme with fourth-order accuracy in time for the TE problems (1.1)–(1.3). Let

$$V = (H_z, E_x, E_y)^T, \tag{2.11}$$

and

$$P = \begin{pmatrix} 0 & 0 & -\frac{1}{\mu} \cdot \delta_x \\ 0 & 0 & 0 \\ -\frac{1}{\varepsilon} \cdot \delta_x & 0 & 0 \end{pmatrix}, \tag{2.12}$$

and

$$Q = \begin{pmatrix} 0 & \frac{1}{\mu}\delta_y & 0 \\ \frac{1}{\varepsilon}\delta_y & 0 & 0 \\ 0 & 0 & 0 \end{pmatrix}. \tag{2.13}$$

The ADI-FDTD method consists of two steps:
Step 1:

$$(I - \frac{\Delta t}{2}P)V^{n+\frac{1}{2}} = (I + \frac{\Delta t}{2}Q)V^n, \tag{2.14}$$

Step 2:

$$(I - \frac{\Delta t}{2}Q)V^{n+1} = (I + \frac{\Delta t}{2}P)V^{n+\frac{1}{2}}, \tag{2.15}$$

where I is a 3×3 identity matrix and u^n and u^{n+1} are the fields at integer time steps. We know that this method is second-order accurate in time. Motivated by the method in [23], we design the new numerical scheme for the TE problems (1.1)–(1.3) as

$$(I - \alpha_1\frac{\Delta t}{2}P)V^{n,1} = (I + \alpha_1\frac{\Delta t}{2}Q)V^n, \tag{2.16}$$

$$(I - \alpha_1\frac{\Delta t}{2}Q)V^{n,2} = (I + \alpha_1\frac{\Delta t}{2}P)V^{n,1}, \tag{2.17}$$

$$(I - \alpha_0\frac{\Delta t}{2}P)V^{n,3} = (I + \alpha_0\frac{\Delta t}{2}Q)V^{n,2}, \tag{2.18}$$

$$(I - \alpha_0\frac{\Delta t}{2}Q)V^{n,4} = (I + \alpha_0\frac{\Delta t}{2}P)V^{n,3}, \tag{2.19}$$

$$(I - \alpha_1\frac{\Delta t}{2}P)V^{n,5} = (I + \alpha_1\frac{\Delta t}{2}Q)V^{n,4}, \tag{2.20}$$

$$(I - \alpha_1\frac{\Delta t}{2}Q)V^{n+1} = (I + \alpha_1\frac{\Delta t}{2}P)V^{n,5}, \tag{2.21}$$

where the coefficients α_0 and α_1 are given by

$$\alpha_0 = \frac{-\sqrt[3]{2}}{2 - \sqrt[3]{2}}, \quad \alpha_1 = \frac{1}{2 - \sqrt[3]{2}}.$$

From [9], we know that the coefficients are determined by

$$\alpha_0 + 2\alpha_1 = 1, \quad \alpha_0^3 + 2\alpha_1^3 = 0.$$

It is easy to prove that the schemes described by (2.16)–(2.21) are unconditionally stable and have fourth-order accuracy in time. In order to analyze the numerical energy of the schemes given by (2.16)–(2.21), we rewrite them as follows:

Stage 1:

$$\begin{cases} H^{n,1}_{z_{i+\frac{1}{2},j+\frac{1}{2}}} + \frac{\alpha_1\Delta t}{2\mu}\delta_x E^{n,1}_{y_{i+\frac{1}{2},j+\frac{1}{2}}} = H^{n}_{z_{i+\frac{1}{2},j+\frac{1}{2}}} + \frac{\alpha_1\Delta t}{2\mu}\delta_y E^{n}_{x_{i+\frac{1}{2},j+\frac{1}{2}}}, \\ E^{n,1}_{x_{i+\frac{1}{2},j}} = E^{n}_{x_{i+\frac{1}{2},j}} + \frac{\alpha_1\Delta t}{2\varepsilon}\delta_y H^{n}_{z_{i+\frac{1}{2},j}}, \\ E^{n,1}_{y_{i,j+\frac{1}{2}}} + \frac{\alpha_1\Delta t}{2\varepsilon}\delta_x H^{n,1}_{z_{i,j+\frac{1}{2}}} = E^{n}_{y_{i,j+\frac{1}{2}}}. \end{cases} \tag{2.22}$$

Stage 2:

$$\begin{cases} H^{n,2}_{z_{i+\frac{1}{2},j+\frac{1}{2}}} - \frac{\alpha_1\Delta t}{2\mu}\delta_y E^{n,2}_{x_{i+\frac{1}{2},j+\frac{1}{2}}} = H^{n,1}_{z_{i+\frac{1}{2},j+\frac{1}{2}}} - \frac{\alpha_1\Delta t}{2\mu}\delta_x E^{n,1}_{y_{i+\frac{1}{2},j+\frac{1}{2}}}, \\ -\frac{\alpha_1\Delta t}{2\varepsilon}\delta y H^{n,2}_{z_{i+\frac{1}{2},j}} + E^{n,2}_{x_{i+\frac{1}{2},j}} = E^{n,1}_{x_{i+\frac{1}{2},j}}, \\ E^{n,2}_{y_{i,j+\frac{1}{2}}} = -\frac{\alpha_1\Delta t}{2\varepsilon}\delta_x H^{n,1}_{z_{i,j+\frac{1}{2}}} + E^{n,1}_{y_{i,j+\frac{1}{2}}}. \end{cases} \tag{2.23}$$

Stage 3:

$$\begin{cases} H^{n,3}_{z_{i+\frac{1}{2},j+\frac{1}{2}}} + \frac{\alpha_0\Delta t}{2\mu}\delta_x E^{n,3}_{y_{i+\frac{1}{2},j+\frac{1}{2}}} = H^{n,2}_{z_{i+\frac{1}{2},j+\frac{1}{2}}} + \frac{\alpha_0\Delta t}{2\mu}\delta_y E^{n,2}_{x_{i+\frac{1}{2},j+\frac{1}{2}}}, \\ E^{n,3}_{x_{i+\frac{1}{2},j}} = E^{n,2}_{x_{i+\frac{1}{2},j}} + \frac{\alpha_0\Delta t}{2\varepsilon}\delta_y H^{n,2}_{z_{i+\frac{1}{2},j}}, \\ E^{n,3}_{y_{i,j+\frac{1}{2}}} + \frac{\alpha_0\Delta t}{2\varepsilon}\delta_x H^{n,3}_{z_{i,j+\frac{1}{2}}} = E^{n,2}_{y_{i,j+\frac{1}{2}}}. \end{cases} \tag{2.24}$$

Stage 4:

$$\begin{cases} H^{n,4}_{z_{i+\frac{1}{2},j+\frac{1}{2}}} - \frac{\alpha_0\Delta t}{2\mu}\delta_y E^{n,4}_{x_{i+\frac{1}{2},j+\frac{1}{2}}} = H^{n,3}_{z_{i+\frac{1}{2},j+\frac{1}{2}}} - \frac{\alpha_0\Delta t}{2\mu}\delta_x E^{n,3}_{y_{i+\frac{1}{2},j+\frac{1}{2}}}, \\ -\frac{\alpha_0\Delta t}{2\varepsilon}\delta y H^{n,4}_{z_{i+\frac{1}{2},j}} + E^{n,4}_{x_{i+\frac{1}{2},j}} = E^{n,3}_{x_{i+\frac{1}{2},j}}, \\ E^{n,4}_{y_{i,j+\frac{1}{2}}} = -\frac{\alpha_0\Delta t}{2\varepsilon}\delta_x H^{n,3}_{z_{i,j+\frac{1}{2}}} + E^{n,3}_{y_{i,j+\frac{1}{2}}}. \end{cases} \tag{2.25}$$

Stage 5:

$$\begin{cases} H^{n,5}_{z_{i+\frac{1}{2},j+\frac{1}{2}}} + \frac{\alpha_1\Delta t}{2\mu}\delta_x E^{n,5}_{y_{i+\frac{1}{2},j+\frac{1}{2}}} = H^{n,4}_{z_{i+\frac{1}{2},j+\frac{1}{2}}} + \frac{\alpha_1\Delta t}{2\mu}\delta_y E^{n,4}_{x_{i+\frac{1}{2},j+\frac{1}{2}}}, \\ E^{n,5}_{x_{i+\frac{1}{2},j}} = E^{n,4}_{x_{i+\frac{1}{2},j}} + \frac{\alpha_1\Delta t}{2\varepsilon}\delta_y H^{n,4}_{z_{i+\frac{1}{2},j}}, \\ E^{n,5}_{y_{i,j+\frac{1}{2}}} + \frac{\alpha_1\Delta t}{2\varepsilon}\delta_x H^{n,5}_{z_{i,j+\frac{1}{2}}} = E^{n,4}_{y_{i,j+\frac{1}{2}}}. \end{cases} \tag{2.26}$$

Stage 6:

$$\begin{cases} H^{n+1}_{z_{i+\frac{1}{2},j+\frac{1}{2}}} - \frac{\alpha_1\Delta t}{2\mu}\delta_y E^{n+1}_{x_{i+\frac{1}{2},j+\frac{1}{2}}} = H^{n,1}_{z_{i+\frac{1}{2},j+\frac{1}{2}}} - \frac{\alpha_1\Delta t}{2\mu}\delta_x E^{n,5}_{y_{i+\frac{1}{2},j+\frac{1}{2}}}, \\ -\frac{\alpha_1\Delta t}{2\varepsilon}\delta y H^{n+1}_{z_{i+\frac{1}{2},j}} + E^{n+1}_{x_{i+\frac{1}{2},j}} = E^{n,5}_{x_{i+\frac{1}{2},j}}, \\ E^{n+1}_{y_{i,j+\frac{1}{2}}} = -\frac{\alpha_1\Delta t}{2\varepsilon}\delta_x H^{n,5}_{z_{i,j+\frac{1}{2}}} + E^{n,5}_{y_{i,j+\frac{1}{2}}}. \end{cases} \tag{2.27}$$

The boundary and initial conditions are given by

$$E^{n}_{x_{i+\frac{1}{2},0}} = E^{n}_{x_{i+\frac{1}{2},J}} = E^{n}_{y_{0,j+\frac{1}{2}}} = E^{n}_{y_{I,j+\frac{1}{2}}} = 0, \qquad 0 \le n \le N, \tag{2.28}$$

and

$$E^{0}_{x_{\alpha,\beta}} = E_{x_0}(\alpha\Delta x, \beta\Delta y), E^{0}_{y_{\alpha,\beta}} = E_{y_0}(\alpha\Delta x, \beta\Delta y), H^{0}_{z_{\alpha,\beta}} = H_{z_0}(\alpha\Delta x, \beta\Delta y). \tag{2.29}$$

3. Energy analysis

The goal of this section is to derive the numerical energy identity of the schemes described by (2.22)–(2.27) and prove that this scheme is unconditionally stable. To this end, we fist prove the following lemma.

Lemma 3.1. *Let $E^n_{y_{i,j+\frac{1}{2}}}$ and $H^n_{z_{i+\frac{1}{2},j+\frac{1}{2}}}$ be the grid function in the ADI-FDTD schemes (2.22)–(2.27) that satisfies the boundary condition (2.1). Then, it holds that*

$$\sum_{i=0}^{I-1}\sum_{j=1}^{J-1} H^n_{z_{i+\frac{1}{2},j+\frac{1}{2}}}\delta_x E^n_{y_{i+\frac{1}{2},j+\frac{1}{2}}} = -\sum_{i=1}^{I-1}\sum_{j=1}^{J-1}\delta_x H^n_{z_{i,j+\frac{1}{2}}} E^n_{y_{i,j+\frac{1}{2}}}.$$

Proof. Using the definition of the operator δ_x, we have

$$\begin{aligned}
&\sum_{i=0}^{I-1}\sum_{j=1}^{J-1} H^n_{z_{i+\frac{1}{2},j+\frac{1}{2}}}\delta_x E^n_{y_{i+\frac{1}{2},j+\frac{1}{2}}}\\
&=\sum_{j=1}^{J-1}(H^n_{z_{\frac{1}{2},j+\frac{1}{2}}}\frac{E_{y^n_{1,j+\frac{1}{2}}}-E_{y^n_{0,j+\frac{1}{2}}}}{\Delta x}+H^n_{z_{\frac{3}{2},j+\frac{1}{2}}}\frac{E_{y^n_{2,j+\frac{1}{2}}}-E_{y^n_{1,j+\frac{1}{2}}}}{\Delta x}+\cdots+H^n_{z_{I-\frac{1}{2},j+\frac{1}{2}}}\frac{E_{y^n_{I,j+\frac{1}{2}}}-E_{y^n_{I-1,j+\frac{1}{2}}}}{\Delta x}).
\end{aligned}$$

The right side term of the above equation becomes

$$\begin{aligned}
&\sum_{j=1}^{J-1}(-\frac{H^n_{z_{\frac{1}{2},j+\frac{1}{2}}}E_{y^n_{0,j+\frac{1}{2}}}}{\Delta x}+\frac{H^n_{z_{\frac{1}{2},j+\frac{1}{2}}}E_{y^n_{1,j+\frac{1}{2}}}}{\Delta x}-\frac{H^n_{z_{\frac{3}{2},j+\frac{1}{2}}}E_{y^n_{1,j+\frac{1}{2}}}}{\Delta x}+\frac{H^n_{z_{\frac{3}{2},j+\frac{1}{2}}}E_{y^n_{2,j+\frac{1}{2}}}}{\Delta x}\\
&+\cdots-\frac{H^n_{z_{I-\frac{1}{2},j+\frac{1}{2}}}E_{y^n_{I-1,j+\frac{1}{2}}}}{\Delta x}+\frac{H^n_{z_{I-\frac{1}{2},j+\frac{1}{2}}}E_{y^n_{I,j+\frac{1}{2}}}}{\Delta x})\\
&=-\sum_{i=1}^{I-1}\sum_{j=1}^{J-1}\delta_x H^n_{z_{i,j+\frac{1}{2}}}E^n_{y_{i,j+\frac{1}{2}}}.
\end{aligned}$$

This completes the proof of Lemma 3.1. □

Next, we use Lemma 3.1 to derive the numerical energy identity for the schemes (2.22)–(2.27) .

Theorem 3.2. *Let $\boldsymbol{E}^n = (E^n_{x_{i+\frac{1}{2},j}}, E^n_{y_{i,j+\frac{1}{2}}})$ and $H^n_{z_{i+\frac{1}{2},j+\frac{1}{2}}}$ be the solutions of the schemes (2.22)–(2.27); then, it holds that*

$$\|\boldsymbol{E}^{n+1}\|^2_E+\|H^{n+1}_z\|^2_{H_z}+\xi=\|\boldsymbol{E}^n\|^2_E+\|H^n_z\|^2_{H_z}+\eta,\qquad 0\le n\le N-1, \tag{3.1}$$

where

$$\begin{aligned}
\xi&=\frac{\Delta t^2}{4\varepsilon\mu}[\alpha_0^2(\|\delta_y E^{n,4}_x\|^2_{\delta_y E_x}+\|\delta_y H^{n,4}_z\|^2_{\delta_y H_z})+\alpha_1^2(\|\delta_y E^{n,2}_x\|^2_{\delta_y E_x}+\|\delta_y H^{n,2}_z\|^2_{\delta_y H_z}+\|\delta_y E^{n+1}_x\|^2_{\delta_y E_x}+\|\delta_y H^{n+1}_z\|^2_{\delta_y H_z})],\\
\eta&=\frac{\Delta t^2}{4\varepsilon\mu}[\alpha_0^2(\|\delta_y E^{n,2}_x\|^2_{\delta_y E_x}+\|\delta_y H^{n,2}_z\|^2_{\delta_y H_z})+\alpha_1^2(\|\delta_y E^{n,4}_x\|^2_{\delta_y E_x}+\|\delta_y H^{n,4}_z\|^2_{\delta_y H_z}+\|\delta_y E^{n}_x\|^2_{\delta_y E_x}+\|\delta_y H^{n}_z\|^2_{\delta_y H_z})].
\end{aligned}$$

Proof. Square both sides of the equations in Stage 1 (2.22), so it is easy to get

$$\begin{cases}
\left(H^{n,1}_{z_{i+\frac{1}{2},j+\frac{1}{2}}}+\alpha_1\frac{\Delta t}{2\mu}\delta_x E^{n,1}_{y_{i+\frac{1}{2},j+\frac{1}{2}}}\right)^2=\left(H^n_{z_{i+\frac{1}{2},j+\frac{1}{2}}}+\alpha_1\frac{\Delta t}{2\mu}\delta_y E^n_{x_{i+\frac{1}{2},j+\frac{1}{2}}}\right)^2,\\
\left(E^{n,1}_{x_{i+\frac{1}{2},j}}\right)^2=\left(E^n_{x_{i+\frac{1}{2},j}}+\alpha_1\frac{\Delta t}{2\varepsilon}\delta_y H^n_{z_{i+\frac{1}{2},j}}\right)^2,\\
\left(E^{n,1}_{y_{i,j+\frac{1}{2}}}+\alpha_1\frac{\Delta t}{2\varepsilon}\delta_x H^{n,1}_{z_{i,j+\frac{1}{2}}}\right)^2=\left(E^n_{y_{i,j+\frac{1}{2}}}\right)^2.
\end{cases} \tag{3.2}$$

We sum over all the terms over all i and j, and then add these equations together, yielding

$$\begin{aligned}&\sum_{i=0}^{I-1}\sum_{j=0}^{J-1}\left(\mu(H^{n,1}_{z_{i+\frac{1}{2},j+\frac{1}{2}}})^2+\alpha_1\Delta t H^{n,1}_{z_{i+\frac{1}{2},j+\frac{1}{2}}}\delta_x E^{n,1}_{y_{i+\frac{1}{2},j+\frac{1}{2}}}+\frac{\alpha_1^2\Delta t^2\varepsilon}{4\varepsilon\mu}(\delta_x E^{n,1}_{y_{i+\frac{1}{2},j+\frac{1}{2}}})^2\right)\\ =&\sum_{i=0}^{I-1}\sum_{j=0}^{J-1}\left(\mu(H^{n}_{z_{i+\frac{1}{2},j+\frac{1}{2}}})^2+\alpha_1\Delta t H^{n}_{z_{i+\frac{1}{2},j+\frac{1}{2}}}\delta_y E^{n}_{x_{i+\frac{1}{2},j+\frac{1}{2}}}+\frac{\alpha_1^2\Delta t^2\varepsilon}{4\varepsilon\mu}(\delta_y E^{n}_{x_{i+\frac{1}{2},j+\frac{1}{2}}})^2\right),\end{aligned}\tag{3.3}$$

and

$$\varepsilon\sum_{i=0}^{I-1}\sum_{j=1}^{J-1}(E^{n,1}_{x_{i+\frac{1}{2},j}})^2=\sum_{i=0}^{I-1}\sum_{j=1}^{J-1}\left(\varepsilon(E^{n}_{x_{i+\frac{1}{2},j}})^2+\frac{\alpha_1^2\Delta t^2\mu}{4\varepsilon\mu}(\delta_y H^{n}_{z_{i+\frac{1}{2},j}})^2+\alpha_1\Delta t E^{n}_{x_{i+\frac{1}{2},j}}\delta_y H^{n}_{z_{i+\frac{1}{2},j}}\right),\tag{3.4}$$

and

$$\varepsilon\sum_{i=1}^{I-1}\sum_{j=0}^{J-1}(E^{n}_{y_{i,j+\frac{1}{2}}})^2=\sum_{i=1}^{I-1}\sum_{j=0}^{J-1}\left(\varepsilon(E^{n,1}_{y_{i,j+\frac{1}{2}}})^2+\frac{\alpha_1^2\Delta t^2\mu}{4\varepsilon\mu}(\delta_x H^{n,1}_{z_{i,j+\frac{1}{2}}})^2+\alpha_1\Delta t\delta_x H^{n,1}_{z_{i,j+\frac{1}{2}}}E^{n,1}_{y_{i,j+\frac{1}{2}}}\right).\tag{3.5}$$

For the above equations given by (3.3)–(3.5), using Lemma 3.1 and the PEC boundary condition, we have

$$\begin{aligned}&\|E^{n,1}_x\|^2_{E_x}+\|E^{n,1}_y\|^2_{E_y}+\|H^{n,1}_z\|^2_{H_z}+\frac{\alpha_1^2\Delta t^2}{4\varepsilon\mu}(\|\delta_x E^{n,1}_y\|^2_{\delta_x E_y}+\|\delta_x H^{n,1}_z\|^2_{\delta_x H_z})\\ =&\|E^{n}_x\|^2_{E_x}+\|E^{n}_y\|^2_{E_y}+\|H^{n}_z\|^2_{H_z}+\frac{\alpha_1^2\Delta t^2}{4\varepsilon\mu}(\|\delta_x E^{n}_y\|^2_{\delta_x E_y}+\|\delta_x H^{n}_z\|^2_{\delta_x H_z}).\end{aligned}\tag{3.6}$$

In a similar way, from the equations in (2.23), we can obtain that

$$\begin{aligned}&\mu\sum_{i=0}^{I-1}\sum_{j=0}^{J-1}(H^{n,2}_{z_{i+\frac{1}{2},j+\frac{1}{2}}})^2+\sum_{i=0}^{I-1}\sum_{j=0}^{J-1}\frac{\alpha_1^2\Delta t^2\varepsilon}{4\varepsilon\mu}(\delta_y E^{n,2}_{x_{i+\frac{1}{2},j+\frac{1}{2}}})^2-\sum_{i=0}^{I-1}\sum_{j=0}^{J-1}\alpha_1\Delta t H^{n,2}_{z_{i+\frac{1}{2},j+\frac{1}{2}}}\delta_y E^{n,2}_{x_{i+\frac{1}{2},j+\frac{1}{2}}}\\ =&\mu\sum_{i=0}^{I-1}\sum_{j=0}^{J-1}(H^{n,1}_{z_{i+\frac{1}{2},j+\frac{1}{2}}})^2+\sum_{i=0}^{I-1}\sum_{j=0}^{J-1}\frac{\alpha_1^2\Delta t^2\varepsilon}{4\varepsilon\mu}(\delta_x E^{n,1}_{y_{i+\frac{1}{2},j+\frac{1}{2}}})-\sum_{i=0}^{I-1}\sum_{j=0}^{J-1}\alpha_1\Delta t H^{n,1}_{z_{i+\frac{1}{2},j+\frac{1}{2}}}\delta_x E^{n,1}_{y_{i+\frac{1}{2},j+\frac{1}{2}}},\end{aligned}\tag{3.7}$$

and

$$\begin{aligned}&\varepsilon\sum_{i=0}^{I-1}\sum_{j=1}^{J-1}(E^{n,1}_{x_{i+\frac{1}{2},j}})^2\\ =&\sum_{i=0}^{I-1}\sum_{j=1}^{J-1}\frac{\alpha_1^2\Delta t^2\mu}{4\varepsilon\mu}(\delta_y H^{n,2}_{z_{i+\frac{1}{2},j}})^2+\varepsilon\sum_{i=0}^{I-1}\sum_{j=1}^{J-1}(E^{n,2}_{x_{i+\frac{1}{2},j}})^2-\sum_{i=0}^{I-1}\sum_{j=1}^{J-1}\alpha_1\Delta t\delta_y H^{n}_{z_{i+\frac{1}{2},j}}E^{n,2}_{x_{i+\frac{1}{2},j}},\end{aligned}\tag{3.8}$$

and

$$\varepsilon\sum_{i=1}^{I-1}\sum_{j=0}^{J-1}(E^{n,2}_{y_{i,j+\frac{1}{2}}})^2$$

$$= \sum_{i=1}^{I-1}\sum_{j=0}^{J-1}\frac{\alpha_1^2\Delta t^2\mu}{4\varepsilon\mu}(\delta_x H_{z_{i,j+\frac{1}{2}}}^{n,2})^2 + \varepsilon\sum_{i=1}^{I-1}\sum_{j=0}^{J-1}(E_{y_{i,j+\frac{1}{2}}}^{n,1})^2 - \sum_{i=1}^{I-1}\sum_{j=0}^{J-1}\alpha_1\Delta t\delta_x H_{z_{i,j+\frac{1}{2}}}^{n,1}E_{y_{i,j+\frac{1}{2}}}^{n,1}. \tag{3.9}$$

We take the sum of (3.7)–(3.9), and get that

$$\begin{aligned}&\|E_x^{n,2}\|_{E_x}^2 + \|E_y^{n,2}\|_{E_y}^2 + \|H_z^{n,2}\|_{H_z}^2 + \frac{\alpha_1^2\Delta t^2}{4\varepsilon\mu}(\|\delta_y E_x^{n,2}\|_{\delta_y E_x}^2 + \|\delta_y H_z^{n,2}\|_{\delta_y H_z}^2)\\ &= \|E_x^{n,1}\|_{E_x}^2 + \|E_y^{n,1}\|_{E_y}^2 + \|H_z^{n,1}\|_{H_z}^2 + \frac{\alpha_1^2\Delta t^2}{4\varepsilon\mu}(\|\delta_x E_y^{n,1}\|_{\delta_x E_y}^2 + \|\delta_x H_z^{n,1}\|_{\delta_x H_z}^2).\end{aligned} \tag{3.10}$$

Similar to the derivation of (3.6), from (2.23) we get

$$\begin{aligned}&\|E_x^{n,3}\|_{E_x}^2 + \|E_y^{n,3}\|_{E_y}^2 + \|H_z^{n,3}\|_{H_z}^2 + \frac{\alpha_0^2\Delta t^2}{4\varepsilon\mu}(\|\delta_x E_y^{n,3}\|_{\delta_x E_y}^2 + \|\delta_x H_z^{n,3}\|_{\delta_x H_z}^2)\\ &= \|E_x^{n,2}\|_{E_x}^2 + \|E_y^{n,2}\|_{E_y}^2 + \|H_z^{n,2}\|_{H_z}^2 + \frac{\alpha_0^2\Delta t^2}{4\varepsilon\mu}(\|\delta_y E_x^{n,2}\|_{\delta_y E_x}^2 + \|\delta_y H_z^{n,2}\|_{\delta_y H_z}^2).\end{aligned} \tag{3.11}$$

Similarly, from (2.24)–(2.27), we also obtain the following identities:

$$\begin{aligned}&\|E_x^{n,4}\|_{E_x}^2 + \|E_y^{n,4}\|_{E_y}^2 + \|H_z^{n,4}\|_{H_z}^2 + \frac{\alpha_0^2\Delta t^2}{4\varepsilon\mu}(\|\delta_y E_x^{n,4}\|_{\delta_y E_x}^2 + \|\delta_y H_z^{n,4}\|_{\delta_y H_z}^2)\\ &= \|E_x^{n,3}\|_{E_x}^2 + \|E_y^{n,3}\|_{E_y}^2 + \|H_z^{n,3}\|_{H_z}^2 + \frac{\alpha_0^2\Delta t^2}{4\varepsilon\mu}(\|\delta_x E_y^{n,3}\|_{\delta_x E_y}^2 + \|\delta_x H_z^{n,3}\|_{\delta_x H_z}^2),\end{aligned} \tag{3.12}$$

and

$$\begin{aligned}&\|E_x^{n,5}\|_{E_x}^2 + \|E_y^{n,5}\|_{E_y}^2 + \|H_z^{n,5}\|_{H_z}^2 + \frac{\alpha_1^2\Delta t^2}{4\varepsilon\mu}(\|\delta_x E_y^{n,5}\|_{\delta_x E_y}^2 + \|\delta_x H_z^{n,5}\|_{\delta_x H_z}^2)\\ &= \|E_x^{n,4}\|_{E_x}^2 + \|E_y^{n,4}\|_{E_y}^2 + \|H_z^{n,4}\|_{H_z}^2 + \frac{\alpha_1^2\Delta t^2}{4\varepsilon\mu}(\|\delta_y E_x^{n,4}\|_{\delta_y E_x}^2 + \|\delta_y H_z^{n,4}\|_{\delta_y H_z}^2),\end{aligned} \tag{3.13}$$

and

$$\begin{aligned}&\|E_x^{n+1}\|_{E_x}^2 + \|E_y^{n+1}\|_{E_y}^2 + \|H_z^{n+1}\|_{H_z}^2 + \frac{\alpha_1^2\Delta t^2}{4\varepsilon\mu}(\|\delta_y E_x^{n+1}\|_{\delta_y E_x}^2 + \|\delta_y H_z^{n+1}\|_{\delta_y H_z}^2)\\ &= \|E_x^{n,5}\|_{E_x}^2 + \|E_y^{n,5}\|_{E_y}^2 + \|H_z^{n,5}\|_{H_z}^2 + \frac{\alpha_1^2\Delta t^2}{4\varepsilon\mu}(\|\delta_x E_y^{n,5}\|_{\delta_x E_y}^2 + \|\delta_x H_z^{n,5}\|_{\delta_x H_z}^2).\end{aligned} \tag{3.14}$$

Take the sum of (3.6)–(3.14), and then we have

$$\begin{aligned}&\|E_x^{n+1}\|_{E_x}^2 + \|E_y^{n+1}\|_{E_y}^2 + \|H_z^{n+1}\|_{H_z}^2 + \frac{\alpha_1^2\Delta t^2}{4\varepsilon\mu}(\|\delta_y E_x^{n,2}\|_{\delta_y E_x}^2 + \|\delta_y H_z^{n,2}\|_{\delta_y H_z}^2)\\ &+ \frac{\alpha_0^2\Delta t^2}{4\varepsilon\mu}(\|\delta_y E_x^{n,4}\|_{\delta_y E_x}^2 + \|\delta_y H_z^{n,4}\|_{\delta_y H_z}^2) + \frac{\alpha_1^2\Delta t^2}{4\varepsilon\mu}(\|\delta_y E_x^{n+1}\|_{\delta_y E_x}^2 + \|\delta_y H_z^{n+1}\|_{\delta_y H_z}^2)\\ &= \|E_x^{n}\|_{E_x}^2 + \|E_y^{n}\|_{E_y}^2 + \|H_z^{n}\|_{H_z}^2 + \frac{\alpha_0^2\Delta t^2}{4\varepsilon\mu}(\|\delta_y E_x^{n,2}\|_{\delta_y E_x}^2 + \|\delta_y H_z^{n,2}\|_{\delta_y H_z}^2)\\ &+ \frac{\alpha_1^2\Delta t^2}{4\varepsilon\mu}(\|\delta_y E_x^{n,4}\|_{\delta_y E_x}^2 + \|\delta_y H_z^{n,4}\|_{\delta_y H_z}^2) + \frac{\alpha_1^2\Delta t^2}{4\varepsilon\mu}(\|\delta_y E_x^{n}\|_{\delta_y E_x}^2 + \|\delta_y H_z^{n}\|_{\delta_y H_z}^2).\end{aligned} \tag{3.15}$$

It shows that the ADI-FDTD schemes (2.22)–(2.27) are approximately energy-preserving. This proof is completed. □

4. Numerical experiments

In this section, we provide some numerical results to verify the numerical performance of the ADI-FDTD schemes (2.16)–(2.21) for the TE models (1.1)–(1.3).

4.1. Example 1

Set $\Omega = [0,1] \times [0,1]$ surrounded by a perfect conductor and consider the TE models (1.1)–(1.3) in a lossless medium with normalized electric permittivity and magnetic permeability, i.e., $\varepsilon = 1$ and $\mu = 1$. The exact solutions of the problems (1.1)–(1.3) are

$$\begin{aligned} E_x(x,y,t) &= -cos(\sqrt{2}\pi t)cos(\pi x)sin(\pi y), \\ E_y(x,y,t) &= cos(\sqrt{2}\pi t)sin(\pi x)cos(\pi y), \\ H_z(x,y,t) &= -\sqrt{2}sin(\sqrt{2}\pi t)cos(\pi x)cos(\pi y). \end{aligned}$$

The drive routines were written in Matlab, and the computation was run using a 2.20 GHz PC with 8 GB RAM and a Windows 10 operating system.

By calculation and simulation, we obtained some numerical results, as shown in Figures 1–9. The parameters were $\Delta t = 1/40$, $\Delta x{=}\Delta y{=}\Delta t^2$ and $T = 1$.

In Figures 1 and 2, we provide the surfaces between the exact solution E_x and the numerical solution E_x^n with $T = 1$. From the figures we can see clearly that the numerical solution behavior can approximate well the exact solution.

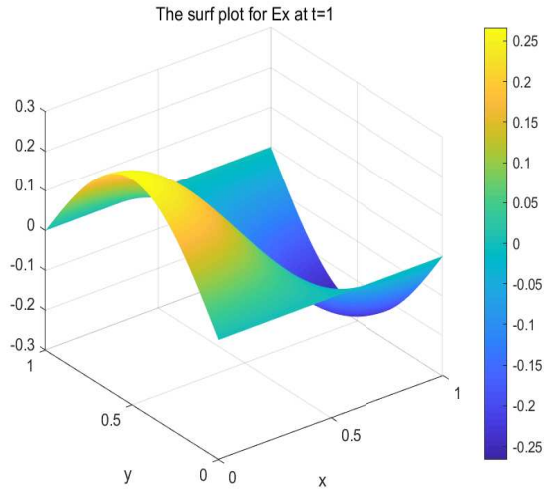

Figure 1. Exact solution E_x.

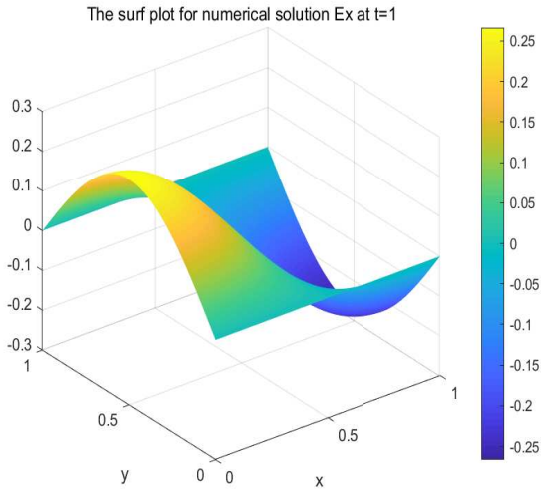

Figure 2. Numerical solution E_x^n.

In Figure 3, the contour of the error $E_x - E_x^n$ is given. We can see clearly that the maximums absolute values of errors were close to 8×10^{-6}, which means that the new scheme is effective for the problems (1.1)–(1.3).

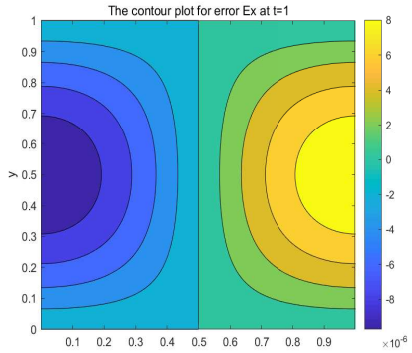

Figure 3. Contour plot for $\ddot{E}_x - E_x^n$ with $T = 1$, $\Delta t = 1/40$.

In addition, we provide the surfaces between the exact solution E_y and the numerical solution E_y^n in Figures 4 and 5, as well as the contour of the error $E_y - E_y^n$ in Figure 6. One can see that the maximums of absolute values of errors were close to 2.3×10^{-5} from Figure 6. From these figures, we can see clearly that the numerical solution E_y^n behavior can approximate well the exact solution E_y.

Similarly, Figures 7 and 8 show the surfaces between the exact solution H_z and the numerical solution H_z^n. The contour of the error $H_z - H_z^n$ is presented in Figure 9; we can see that the maximums of absolute values of errors were close to 1.25×10^{-5}. From these results, it is clear that the numerical solution H_z^n behavior can approximate well the exact solution H_z.

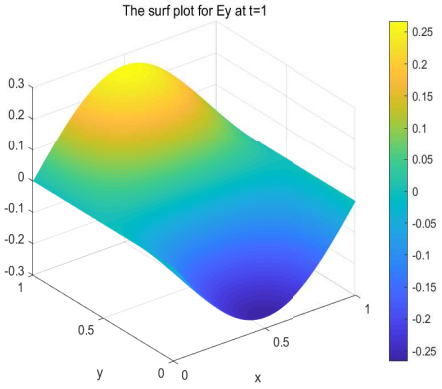

Figure 4. Exact solution E_y.

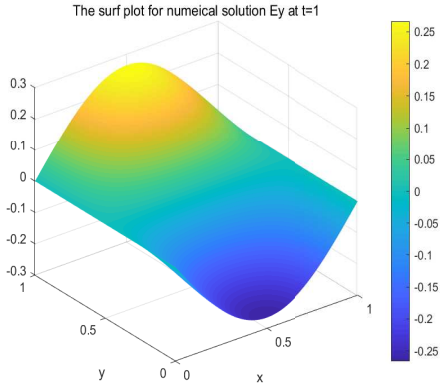

Figure 5. Numerical solution E_y^n.

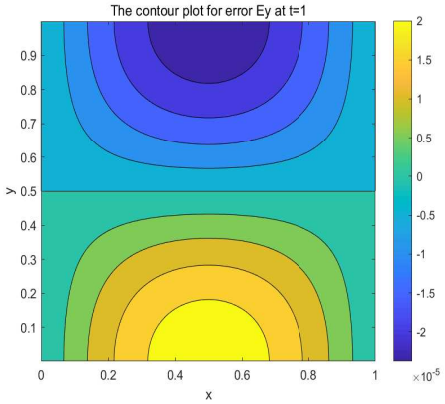

Figure 6. Contour plot for $E_y - E_y^n$ with $T = 1$, $\Delta t = 1/40$.

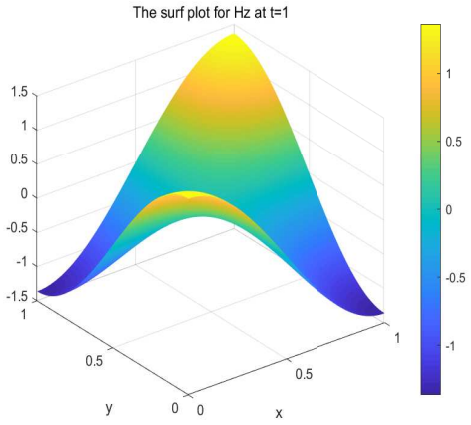

Figure 7. Exact solution Hz.

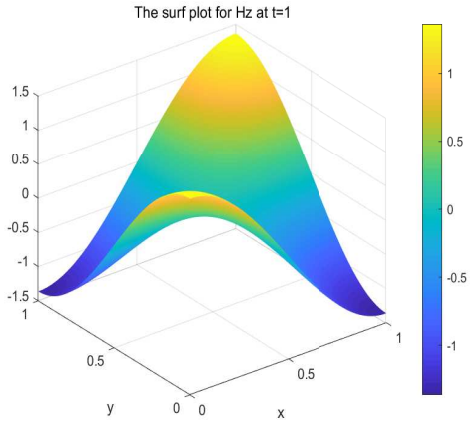

Figure 8. Numerical solution H_z^n.

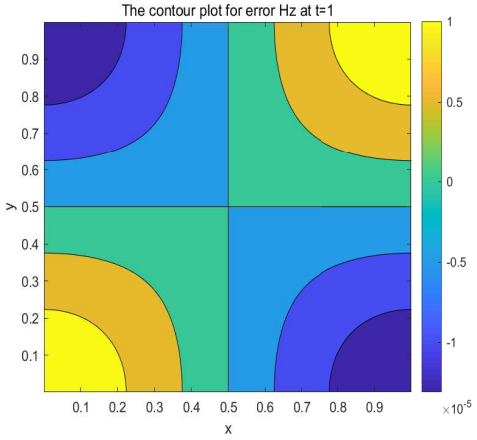

Figure 9. Contour plot for $H_z - H_z^n$ at with $T = 1$, $\Delta t = 1/40$.

In the following, we continue to describe some experiments to test the stability, convergence and energy conservation ability of the ADI-FDTD schemes (2.16)–(2.21). Let $ErrE$ and $ErrH$ be defined by

$$||ErrE||_E^2 = \sum_{i=0}^{I-1}\sum_{j=1}^{J-1} \varepsilon(E_x(i+\frac{1}{2}, j, t_n) - E^n_{x_{i+\frac{1}{2},j}})^2 \Delta x \Delta y, + \sum_{i=1}^{I-1}\sum_{j=0}^{J-1} \varepsilon(E_y(i, j+\frac{1}{2}, t_n) - E^n_{y_{i,j+\frac{1}{2}}})^2 \Delta x \Delta y,$$

$$||ErrH||_{H_z}^2 = \sum_{i=0}^{I-1}\sum_{j=0}^{J-1} \mu(H_z(i+\frac{1}{2}, j+\frac{1}{2}, t_n) - H^n_{z_{i+\frac{1}{2},j+\frac{1}{2}}})^2 \Delta x \Delta y,$$

$$I_{n+1} = (||\mathbf{E}^{n+1}||_E^2 + ||H_z^{n+1}||_{H_z}^2 + \xi)^{1/2},$$

$$I_n = (||\mathbf{E}^{n}||_E^2 + ||H_z^{n}||_{H_z}^2 + \eta)^{1/2},$$

$$E1 = \max_{1\le n\le N-1} ((||\mathbf{E}^{n+1}||_E^2 + ||H_z^{n+1}||_{H_z}^2)^{1/2} - (||\mathbf{E}^{n}||_E^2 + ||H_z^{n}||_{H_z}^2))^{1/2},$$

$$E2 = \max_{1\le n\le N-1} |I_{n+1} - I_n|,$$

where $E_x(i+\frac{1}{2}, j, t_n)$, $E_y(i, j+\frac{1}{2}, t_n)$ and $H_z(i+\frac{1}{2}, j+\frac{1}{2}, t_n)$ are the exact solutions of the problems (1.1)–(1.3) and $E^n_{x_{i+\frac{1}{2},j}}, E^n_{y_{i,j+\frac{1}{2}}}, H^n_{z_{i+\frac{1}{2},j+\frac{1}{2}}}$ are the solutions of the ADI-FDTD methods (2.16)–(2.21) for $n \geq 0$. I^2_{n+1} is the left side of the identity (3.1) and I^2_n is the right side of the identity (3.1). E_1 is the energy difference between the $n+1$ and n levels. E_2 is the difference between the two sides of the Eq (3.1).

In calculation, we take $\Delta x = \Delta y = (\Delta t)^2$, $T = 1$ and $T = 2$. Tables 1 and 2 give the errors of the numerical solution of (1.1)–(1.3) as computed by the ADI-FDTD methods described by (2.16)–(2.21) in the discrete L^2 norms and given convergence rates in different time step sizes $\Delta t = T/N$.

Table 1. Convergence rates of $ErrE$ and $ErrH$ by time step, with $T = 1$.

N	$ErrE$	$Rate$	$ErrH$	$Rate$
5	3.705969E-02		1.879096E-02	
10	2.987580E-03	3.63	1.511953E-03	3.64
20	2.013062E-04	3.90	1.0247E-004	3.88
40	1.283300E-05	3.97	6.5455E-006	3.97
80	8.060774E-07	3.99	4.114049E-07	3.99

Table 2. Convergence rates of $ErrE$ and $ErrH$ by time step, with $T = 2$.

N	$ErrE$	$Rate$	$ErrH$	$Rate$
5	4.141165E-01		2.508505E-01	
10	4.272966E-02	3.28	4.959246E-02	2.34
20	3.309908E-03	3.70	4.254614E-03	3.54
40	2.219418E-04	3.90	2.897803E-04	3.88
80	1.413955E-05	3.97	1.851503E-05	3.97

Tables 3 and 4 give the energy difference between the level n and level $n+1$ in the discrete L^2 norm and the difference between the two sides of the identity given by (3.1).

Table 5 shows the results for $I_n - I_0$, E_1 and E_2 for the spatial steps $\Delta x = \Delta y = 0.01$ and time step of $\Delta t = 0.001$.

Table 3. Energy errors with $T = 1$.

N	E_1	E_2
5	1.017911E-02	1.525899E-03
10	4.667802E-04	1.859628E-05
20	1.655990E-05	1.656034E-07
40	5.326041E-07	1.331381E-09
80	1.677347E-08	1.111833E-11

Table 4. Energy errors with $T = 2$.

N	E_1	E_2
5	1.134799E-01	1.533521E-02
10	1.020233E-02	3.836721E-04
20	4.734900E-04	4.716336E-06
40	1.656010E-05	4.140171E-08
80	5.328719E-07	3.351354E-10

Table 5. Energy errors when $\Delta t = 0.001$ and $\Delta x = \Delta y = 0.01$.

n	100	200	400	1000	2000	4000
I_n-I_0	1.045597E-06	3.62990E-06	5.478538E-06	5.301066E-06	1.518304E-06	4.448625E-06
E_1	4.274359E-14	5.534462E-14	5.534462E-14	5.534462E-14	5.534462E-14	5.534462E-14
E_2	1.665334E-15	2.442491E-15	2.442491E-15	2.664535E-15	2.664535E-15	2.775558E-15

From the numerical results in Tables 1–5, we get the following observations:

- Tables 1 and 2 show the errors and convergence rates with $T = 1$ and $T = 2$. We can see that the ADI-FDTD schemes (2.22)–(2.27) are efficient and have fourth-order accuracy in time.
- Tables 3 and 4 show the energy error between layer n and $n + 1$ and the difference between the left and right sides of the equation (3.1) with $T = 1$, $T = 2$. From the tables, we can see that E_1 and E_2 tend to zero, which verifies the theoretical results in Theorem 3.2.
- Table 5 shows the values of $I_n - I_0$, E_1 and E_2 at $n = 100, 200, 400, 800, 1000, 2000$ and 4000. From the second line we can see that the ADI-FDTD schemes (2.22)–(2.27) are stable and approximately energy-preserving. The third line shows the energy error between layer n and $n + 1$; we can see that the values of E_1 were close to 5.5×10^{-14}. The fourth line shows that the difference between the left and right sides of the equation defined by (3.1) was close to 10^{-15}, which verifies Theorem 3.2.

4.2. Example 2

Set $\Omega = [0, 1] \times [0, 1]$, $k_x = 1$, $k_y = 2$, $\varepsilon = \mu = 1$; the exact solutions of the problems (1.1)–(1.3) are

$$E_x(x, y, t) = \frac{2}{\sqrt{5}} cos(\sqrt{5}\pi t) cos(\pi x) sin(2\pi y),$$
$$E_y(x, y, t) = -\frac{1}{\sqrt{5}} cos(\sqrt{5}\pi t) sin(\pi x) cos(2\pi y),$$
$$H_z(x, y, t) = sin(\sqrt{5}\pi t) cos(\pi x) cos(2\pi y).$$

This example is presented for studying error estimates of the schemes (2.16)–(2.21) with $k_x \neq k_y$. The parameters were $\Delta t = 1/40$, $\Delta x = \Delta y = \Delta t^2$ and $T = 1$. All calculation results are shown in Figures 10–18.

In Figures 10 and 11, we provide the surfaces between the exact solution E_x and the numerical solution E_x^n with $t = 1$. From the figures we can see clearly that the numerical solution behavior can approximate well the exact solution.

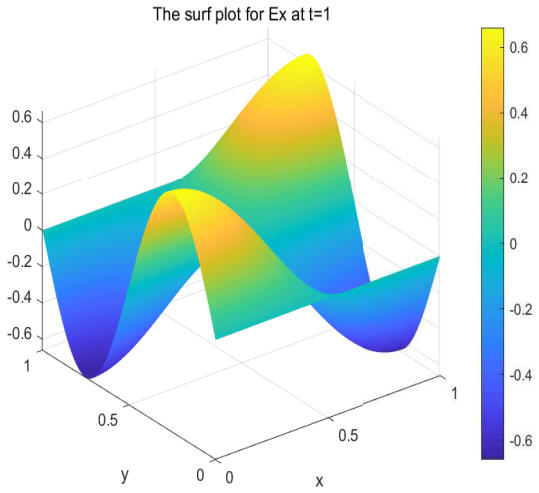

Figure 10. Exact solution E_x.

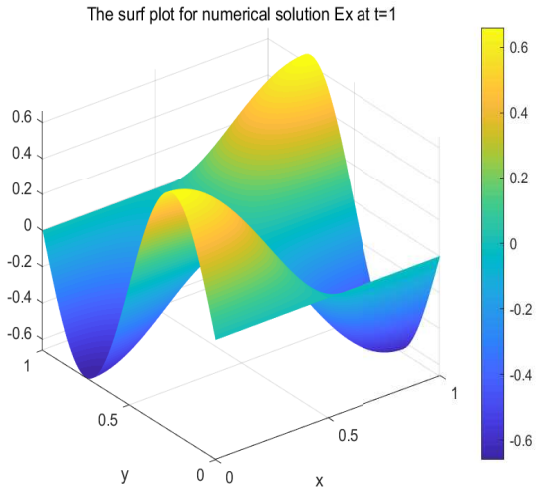

Figure 11. Numerical solution E_x^n.

The contour of the error $E_x - E_x^n$ is presented in Figure 12. One can see that the maximums of absolute values of errors was close to 1.64×10^{-4}, i.e., the new schemes (2.16)–(2.21) are effective for the problems (1.1)–(1.3).

In addition, we provide the surfaces between the exact solution E_y in Figure 13 and the numerical solution E_y^n in Figure 14, as well as the contour of the error $E_y - E_y^n$ in Figure 15. One can see that the maximums of absolute values of errors was close to 6.92×10^{-5} from this Figure 15. From these figures we can see clearly that the numerical solution E_y^n behavior can approximate well the exact solution E_y.

Similarly, Figures 16 and 17 show the surfaces between the exact solution H_z and the numerical solution H_z^n. Figure 18 shows the contour of the error $H_z - H_z^n$, we can see that the maximums of absolute values of errors was close to 2.07×10^{-4}. From these figures we can see clearly that the numerical solution H_z^n behavior can approximate well the exact solution H_z, i.e., the the numerical schemes (2.16)–(2.21) are efficient.

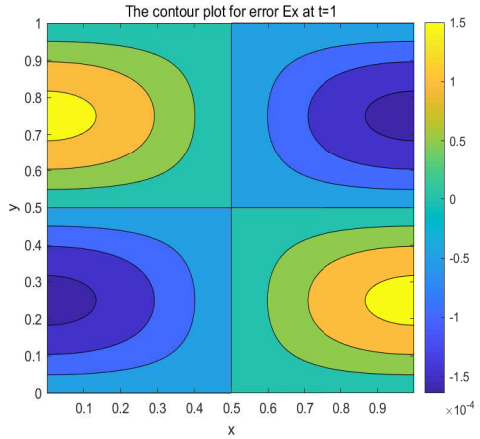

Figure 12. Contour plot for $E_x - E_x^n$ with $T = 1$, $\Delta t = 1/40$.

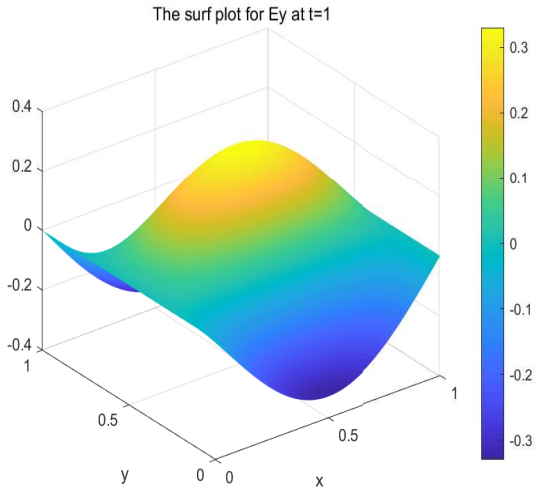

Figure 13. Exact solution E_y.

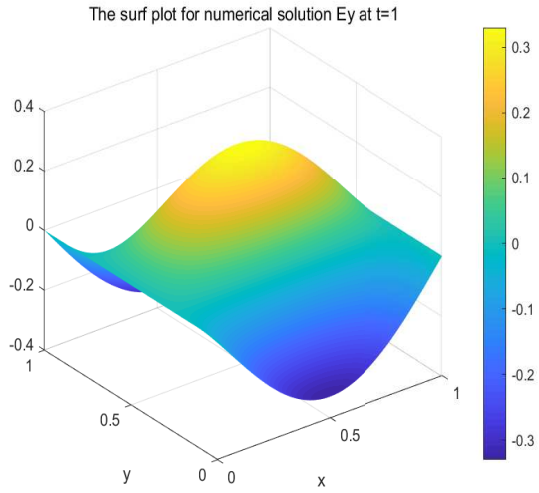

Figure 14. Numerical solution E_y^n.

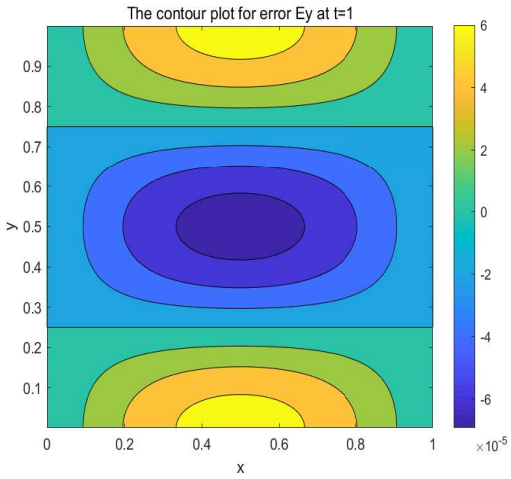

Figure 15. Contour plot for $E_y - E_y^n$ with $T = 1$, $\Delta t = 1/40$.

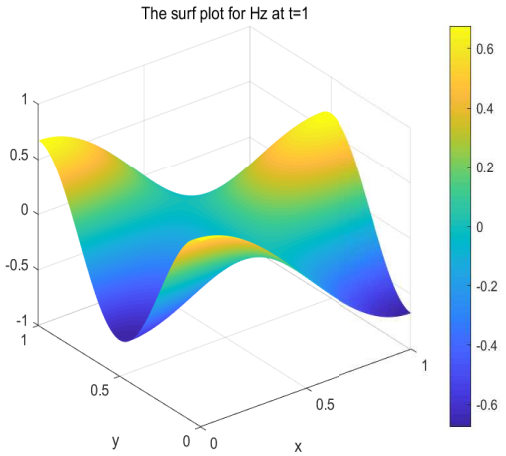

Figure 16. Exact solution Hz.

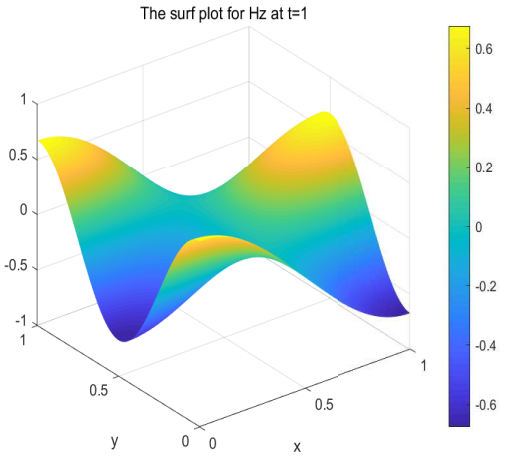

Figure 17. Numerical solution H_z^n.

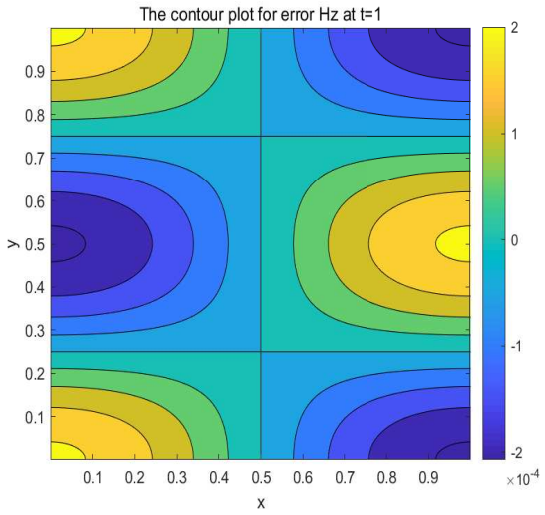

Figure 18. Contour plot for $H_z - H_z^n$ with $T = 1$, $\Delta t = 1/40$.

Furthermore, taking $\Delta x = \Delta y = (\Delta t)^2$ and $T = 1$, some calculation results are shown in Tables 6 and 7. Table 6 shows the error of the numerical solution of (1.1)–(1.3) as computed by using (2.16)–(2.21) in the discrete L^2 norms and convergence rates in different time step sizes $\Delta t = T/N$. The results in Table 6, clearly show that the method is efficient and has fourth-order accuracy in time. E_1 which is the difference in energy between level n and level $n + 1$ and E_2 which is the difference between the two sides of the identity (3.1) are presented in Table 7. The results of E_1 and E_2 in Table 7 verify the theoretical results in Theorem 3.2.

Let E_3 be defined by

$$E_3 = ((\|\mathbf{E}^n\|_E^2 + \|H_z^n\|_{H_z}^2)^{1/2} - (\|\mathbf{E}^0\|_E^2 + \|H_z^0\|_{H_z}^2))^{1/2},$$

we show the errors E_1, E_2 and E_3 in Table 8 with $\Delta x = \Delta y = 0.01$ and $\Delta t = 0.001$. It is clearly shown that for a long time, the numerical solution of the schemes (2.16)–(2.21) keep the approximate energy-preserving nature in the discrete energy norms and are consistent with the theoretical results obtained in Theorem 3.2.

Table 6. Convergence rates of ErrE and ErrH by time step, with $T = 1$.

N	*ErrE*	*Rate*	*ErrH*	*Rate*
5	1.060494E-01		1.856493E-01	
10	1.669285E-02	2.67	2.029985E-02	3.20
20	1.338319E-03	3.64	1.559344E-03	3.70
40	8.913728E-05	3.90	1.035249E-04	3.91
80	5.660689E-06	3.97	6.573273E-05	3.97

Table 7. Energy errors with $T = 1$.

N	E_1	E_2
5	1.685892E-02	9.258177E-03
10	1.183114E-03	1.827276E-04
20	4.861785E-05	1.945590E-06
40	1.656051E-06	1.656084E-08
80	5.280528E-08	1.323115E-10

Table 8. Energy errors when $\Delta t = 0.001$ and $\Delta x = \Delta y = 0.01$.

n	100	200	400	1000	2000	4000
E_1	1.715294E-13	1.742217E-13	1.742217E-13	1.742773E-13	1.743050E-13	1.743050E-13
E_2	2.742251E-14	2.786660E-14	2.797762E-14	2.797762E-14	2.797762E-14	2.808864E-14
E_3	1.035361E-11	2.412220E-11	2.642497E-12	1.132772E-11	2.466771E-11	9.283129E-13

5. Conclusions

In this paper, an ADI-FDTD method with fourth-order accuracy in time for the 2-D TE problem without sources and charges has been proposed and the numerical identity of the method has been derived. It is strictly proved that the proposed method is approximately energy-preserving, and that the two perturbation terms in the energy identity will affect the energy conservation in theory. Numerical experiments to compute the energies and convergence orders in time were carried out, and the computed results confirmed the theoretical analysis. The perturbation terms derived can be used to improve the application of the ADI-FDTD scheme.

Acknowledgments

This work was supported by the National Natural Science Foundation of China (Grant Nos. 11871138, 11801389, 11771314, 12171343), Sichuan Science and Technology Program (Grant Nos. 2020YJ0110, 2022JDTD0019), National-Local Joint Engineering Laboratory of System Credibility Automatic Verification (Grant No. ZD20220105) and funding from the V. C. and V. R. Key Lab of Sichuan Province.

Conflict of interest

The authors declare that they have no conflict of interest.

References

1. K. S. Yee, Numerical solution of inition of initial boundary value problems involving Maxwell's equations in isotropic media, *IEEE T. Antenn. Propag.,* **14** (1966), 302–307. http://dx.doi.org/10.1109/TAP.1966.1138693

2. T. Namiki, A new FDTD algorithm based on alternating direction implicit method, *IEEE T. Microw. Theory,* **47** (1999), 2003–2007. http://dx.doi.org/10.1109/22.795075

3. P. Ciarlet, J. Zou, Fully discrete finite element approaches for time-dependent Maxwell's equations, *Numer. Math.,* **82** (1999), 193–219. http://dx.doi.org/10.1007/s002110050417

4. L. Mu, J. Wang, X. Ye, S. Zhang, A weak Galerkin finite element method for the Maxwell's equations, *J. Sci. Comput.,* **65** (2016), 363–386. http://dx.doi.org/10.1007/s10915-014-9964-4

5. A. Taflove, M. E. Brodwin, Numerical solution of steady-state electromagnetic scattering problems using the time-dependent Maxwell's equations, *IEEE T. Microw. Theory,* **23** (1975), 623–630. http://dx.doi.org/10.1109/tmtt.1975.1128640

6. J. E. Dendy, G. Fairweather, Alternating-direction Galerkin methods for parabolic and hyperbolic problems on rectangular polygons, *SIAM J. Numer. Anal.,* **12** (1975), 144–163. http://dx.doi.org/10.2307/2156287

7. R. Holland, Implicit three-dimensinal finite differencing of Maxwell's equations, *IEEE T. Nucl. Sci.,* **31** (1984), 1322–1326. http://dx.doi.org/10.1109/tns.1984.4333504

8. R. Leis, *Initial boundary value problems in mathematical physics*, New York, Wiley, 1986. http://dx.doi.org/10.1007/978-3-663-10649-4

9. H. Yoshida, Construction of higher order symplectic integrators, *Phys. Lett. A,* **150** (1990), 262–268. http://dx.doi.org/10.1016/0375-9601(90)90092-3

10. S. Li, L. Vu-Quoc, Finite difference calculus invariant structure of a class of algorithms for the nonlinear Klein-Gordon equation, *SIAM J. Numer. Anal.,* **32** (1995), 1839–1875. http://dx.doi.org/10.2307/2158531

11. A. Taflove, S. Hagness, *Computational electrodynamics: The finite-difference time-domain method*, 2Eds., Boston, Artech House, 2000. http://dx.doi.org/10.1016/0021-9169(96)80449-1

12. F. Zheng, Z. Chen, J. Zhang, Toward the development of a three-dimensional unconditionally stable finite-difference time-domain method, *IEEE T. Microw. Theory,* **48** (2000), 1550–1558. http://dx.doi.org/10.1109/22.869007

13. T. Namiki, K. Ito, Investigation of numerical errors of the two-dimensional ADI-FDTD method, *IEEE T. Microw. Theory,* **48** (2000), 1950–1956. http://dx.doi.org/10.1109/22.883876

14. F. Zheng, Z. Chen, Numerical dispersion analysis of the unconditionally stable 3-D ADI-FDTD method, *IEEE T. Microw. Theory,* **49** (2001), 1006–1009. http://dx.doi.org/10.1109/22.920165

15. S. D. Gedney, G. Liu, J. A. Roden, A. Zhu, Perfectly matched layer media with CFS for an unconditional stable ADI-FDTD method, *IEEE T. Antenn. Propag.,* **49** (2001), 1554–1559. http://dx.doi.org/10.1109/8.964091

16. J. Douglas, S. Kim, Improved accuracy for locally one-dimensional methods for parabolic equations, *Math. Mod. Method. Appl. S.,* **11** (2001), 1563–1579. http://dx.doi.org/10.1142/s0218202501001471

17. A. P. Zhao, Analysis of the numerical dispersion of the 2-D alternating-direction implicit FDTD method, *IEEE T. Microw. Theory,* **50** (2002), 1156–1164. http://dx.doi.org/10.1109/22.993419

18. Z. Q. Xie, C. H. Chan, B. Zhang, An explict four-order staggered finite-difference time-domain method for Maxwell's equations, *J. Comput. Appl. Math.,* **147** (2002), 75–98. http://dx.doi.org/10.1016/S0377-0427(02)00394-1

19. L. Gao, B. Zhang, D. Liang, The splitting finite-difference time-domain methods for Maxwell's equations in two dimensions, *J. Comput. Appl. Math.,* **205** (2007), 207–230. http://dx.doi.org/10.1016/j.cam.2006.04.051

20. B. Li, W. Sun, Unconditional convergence and optimal error estimates of a Galerkin-mixed FEM for incompressible miscible flow in porous media, *SIAM J. Numer. Anal.,* **51** (2013), 1959–1977. http://dx.doi.org/10.1137/120871821

21. J. Wang, A new error analysis of Crank-Nicolson Galerkin FEMs for a generalized nonlinear Schrödinger equation, *J. Sci. Comput.,* **60** (2014), 390–407. http://dx.doi.org/10.1007/s10915-013-9799-4

22. D. Li, J. Wang, Unconditionally optimal error analysis of Crank-Nicolson Galerkin FEMs for a strongly nonlinear parabolic system, *J. Sci. Comput.,* **72** (2017), 892–915. http://dx.doi.org/10.1007/s10915-017-0381-3

23. E. L. Tan, Y. H. Ding, ADI-FDTD Method with fourth order accuracy in time, *IEEE T. Microw. Theory,* **18** (2008), 296–298. http://dx.doi.org/10.1109/lmwc.2008.922099

24. W. Chen, X. Li, D. Liang, Energy-conserved splitting FDTD methods for Maxwell's equations, *Numer. Math.,* **108** (2008), 445–485. http://dx.doi.org/10.1007/s00211-007-0123-9

25. W. Chen, X. Li, D. Liang, Symmetric energy-conserved splitting FDTD scheme for the Maxwell's equations, *Commun. Comput. Phys.,* **6** (2009), 804–825. http://dx.doi.org/10.4208/cicp.2009.v6.p804

26. W. Li, D. Liang, Symmetric energy-conserved S-FDTD scheme for two-dimensional Maxwell's equations in negative index metamaterials, *J. Sci. Comput.,* **69** (2016), 696–735. http://dx.doi.org/10.1007/s10915-016-0214-9

27. M. H. Carpenter, D. Gottlieb, S. Abarbanel, Time-stable boundary conditions for finite-difference schemes solving hyperbolic systems: Methodology and application to high-order compact schemes, *J. Comput. Phys.,* **111** (1994), 220–236. http://dx.doi.org/10.1006/jcph.1994.1057

28. D. Appelö, V. A. Bokil, Y. Cheng, F. Li, Energy stable SBP-FDTD methods for Maxwell-Duffing models in nonlinear photonics, *IEEE J. Multiscale Mu.,* **4** (2019), 329–336. http://dx.doi.org/10.1109/jmmct.2019.2959587

29. N. Sharan, P. T. Brady, D. Livescu, Time stability of strong boundary conditions in finite-difference schemes for hyperbolic systems, *SIAM J. Numer. Anal.,* **60** (2022), 1331–1362. http://dx.doi.org/10.1137/21M1419957

30. D. Liang, Q. Yuan, The spatial fourth-order energy-conserved S-FDTD scheme for Maxwell's equations, *J. Comput. Phys.,* **243** (2013), 344–364. http://dx.doi.org/10.1016/j.jcp.2013.02.040

31. L. Gao, X. Li, W. Chen, New energy identities and super convergence analysis of the energy conserved splitting FDTD methods for 3D Maxwell's equations, *Math. Meth. Appl. Sci.,* **36** (2013), 440–455. http://dx.doi.org/10.1002/mma.2605

32. L. Gao, M. Cao, R. Shi, H. Guo, Energy conservation and super convergence analysis of the EC-S-FDTD schemes for Maxwell's equations with periodic boundaries, *Numer. Meth. Part. D. E.,* **35** (2019), 1562–1587. http://dx.doi.org/10.1002/num.22364

33. J. Xie, D. Liang, Z. Zhang, Energy-preserving local mesh-refined splitting FDTD schemes for two dimensional Maxwell's equations, *J. Comput. Phys.,* **425** (2021), 109896. http://dx.doi.org/10.1016/j.jcp.2020.109896

34. D. Wang, A. Xiao, W. Yang, A linearly implicit conservative difference scheme for the space fractional coupled nonlinear Schrödinger equations, *J. Comput. Phys.,* **272** (2014), 644–655. http://dx.doi.org/10.1016/j.jcp.2014.04.047

35. P. Wang, C. Huang, An energy conservative difference scheme for the nonlinear fractional Schrödinger equations, *J. Comput. Phys.,* **293** (2015), 238–251. http://dx.doi.org/10.1016/j.jcp.2014.03.037

36. M. Ran, C. Zhang, A conservative difference scheme for solving the strongly coupled nonlinear fractional Schrödinger equations, *Commun. Nonlinear Sci.,* **41** (2016), 64–83. http://dx.doi.org/10.1016/j.cnsns.2016.04.026

37. M. Ran, C. Zhang, A linearly implicit conservative scheme for the fractional nonlinear Schrödinger equation with wave operator, *Int. J. Comput. Math.,* **93** (2016), 1103–1118. http://dx.doi.org/10.1080/00207160.2015.1016924

38. H. Li, Y. Wang, Q. Sheng, An energy-preserving Crank-Nicolson Galerkin method for Hamiltonian partial differential equations, *Numer. Meth. Part. D. E.,* **32** (2016), 1485–1504. http://dx.doi.org/10.1002/num.22062

AIMS Press